LONG-TIME BEHAVIOR OF NUMERICAL SOLUTIONS TO NONLINEAR FRACTIONAL ODES

Dongling Wang[1], Aiguo Xiao[2] and Jun Zou[3,*]

Abstract. In this work, we study the long time behavior, including asymptotic contractivity and dissipativity, of the solutions to several numerical methods for fractional ordinary differential equations (F-ODEs). The existing algebraic contractivity and dissipativity rates of the solutions to the scalar F-ODEs are first improved. In order to study the long time behavior of numerical solutions to fractional backward differential formulas (F-BDFs), two crucial analytical techniques are developed, with the first one for the discrete version of the fractional generalization of the traditional Leibniz rule, and the other for the algebraic decay rate of the solution to a linear Volterra difference equation. By means of these auxiliary tools and some natural conditions, the solutions to F-BDFs are shown to be contractive and dissipative, and also preserve the exact contractivity rate of the continuous solutions. Two typical F-BDFs, based on the Grünwald–Letnikov formula and L1 method respectively, are studied. For high order F-BDFs, including convolution quadrature schemes based on classical second order BDF and product integration schemes based on quadratic interpolation approximation, their numerical contractivity and dissipativity are also developed under some slightly stronger conditions. Numerical experiments are presented to validate the long time qualitative characteristics of the solutions to F-BDFs, revealing very different decay rates of the numerical solutions in terms of the the initial values between F-ODEs and integer ODEs and demonstrating the superiority of the structure-preserving numerical methods.

1. Introduction

Fractional calculus has been widely applied to many areas in science and engineering. Various fractional-order dynamical models have been proposed in applications, and their numerical solutions have shown better consistencies with experimental data than those produced by the corresponding integer-order differential equations [28, 39, 40]. A typical model is the time fractional anomalous diffusion equation, which describes a diffusion process where the mean square displacement of a particle grows slower or faster than that in the normal diffusion

[1] Department of Mathematics and Center for Nonlinear Studies, Northwest University, 710075 Xi'an, Shaanxi, P.R. China.

[2] Hunan Key Laboratory for Computation and Simulation in Science and Engineering, Xiangtan University, 411105 Xiangtan, Hunan, P.R. China.

[3] Deptartment of Mathematics, The Chinese University of Hong Kong, Shatin, NT, Hong Kong.

*Corresponding author: zou@math.cuhk.edu.hk

process. Anomalous diffusions were observed and confirmed in many experiments. Solutions to fractional anomalous diffusion equations demonstrate an important so-called long-tail effect, that is, they decay asymptotically in an algebraic decay rate, which is generally much slower than the exponential decay rate of classical integer order equations and thus the solutions look like having a long tail geometrically. It is highly interesting and important both mathematically and practically if we could have a quantitative understanding of the long-time dynamical behavior of the solutions to nonlinear fractional models, especially of how the numerical solutions decay and if they can preserve the exact same algebraic decay rate as their continuous counterparts. This is a challenging topic and has basically still not been investigated in the literature, and will be the main motivation and focus of the current work. Let us start with the model of our main interest. For $0 < \alpha < 1$, we consider the Caputo F-ODEs:

$$_0^C D_t^\alpha x(t) = f(t, x(t)), \quad t > 0, \ x \in \mathbb{R}^d, \tag{1.1}$$

with initial condition $x(0) = x_0$, where the Caputo fractional derivative is given by

$$_0^C D_t^\alpha x(t) = \frac{1}{\Gamma(1-\alpha)} \int_0^t \frac{x'(s)}{(t-s)^\alpha} \mathrm{d}s.$$

The stability analysis of F-ODEs has attracted a great attention and the main difficulty in the analysis lies in the nonlocal nature of fractional derivatives. A fundamental stability result for linear F-ODEs, *i.e.*, $f(t, x) = Ax$ for a matrix $A \in \mathbb{R}^{d \times d}$ in (1.1), was established by Matignon [37], where the stability region and a concrete long time algebraic decay rate, namely $O(t^{-\alpha})$ as $t \to +\infty$, of the solutions were derived.

For a linear fractional order integro-differential equation, the asymptotic behavior of continuous and discrete solutions with optimal decay rate $O(t^{-\alpha})$ was derived by constructing a nice contour integral [9]. Many important results and various analytical strategies for the stability of fractional linear systems have been developed in succession; see the survey article [31].

For the stability of nonlinear F-ODEs, a popular approach is to extend the classical Lyapunov theorem to fractional systems and make use of the fractional comparison principle. The concept of the Mittag-Leffler stability and the fractional Lyapunov second method were developed in [32]. This method relies on an appropriate Lyapunov function and the calculation of the Caputo fractional derivative of the function. Under the classical Lipschitz hypothesis on function f, the stability with respect to initial values and the structural stability of F-ODEs were studied in [13]. The stability theory of nonlinear F-ODEs is still far from maturity due to the coupling between the complex structure of the nonlinear function f and the nonlocal feature of fractional derivatives. To illustrate the motivation of the contractivity and dissipativity of solutions to nonlinear F-ODEs, we first recall some relevant results for the classical ODEs, namely,

$$\frac{\mathrm{d}}{\mathrm{d}t} x(t) = f(t, x), \quad x \in \mathbb{R}^d, \tag{1.2}$$

which are assumed to have a unique solution $x \in C[[t_0, +\infty), \mathbb{R}^d]$ for any given initial value $x(t_0) = x_0$.

In order to extend the concept of A-stability for linear multistep methods from the linear test equation to nonlinear systems, Dahlquist [11] introduced the one-sided Lipschitz condition in 1975 for the ODEs (1.2):

$$\langle f(t, x) - f(t, y), \ x - y \rangle \le \lambda \|x - y\|^2, \ \text{for all } x, y \in \mathbb{R}^d, \tag{1.3}$$

where λ is the one-sided Lipschitz constant, $\langle \cdot, \cdot \rangle$ is the Euclidean inner product in $\mathbb{R}^d$, and $\|\cdot, \cdot\|$ is the standard Euclidean norm. This convention is assumed throughout the paper.

Then any two solutions $x(t)$ and $y(t)$ of equation (1.2) with different initial values x_0 and y_0 meet the following stability estimate:

$$\|x(t) - y(t)\| \le \|x_0 - y_0\| \cdot e^{\lambda(t - t_0)}. \tag{1.4}$$

This implies the contractivity and exponential stability of the solutions to the ODEs (1.2) with respect to the initial values for $\lambda \le 0$ and $\lambda < 0$ respectively.

The one-sided Lipschitz condition (1.3) has a significant influence on the numerical methods for stiff ODEs [4, 20]. Stiff problems usually have large classical Lipschitz constant, but there may be a moderately sized, or even a negative one-sided Lipschitz constant. One class of important examples of stiff ODEs are derived from the space discretization of some parabolic equations such as reaction diffusion equations. Dahlquist [11] proposed the concept of G-stability for one-leg methods and the corresponding linear multistep methods (LMMs) for stiff ODEs satisfying the one-sided Lipschitz condition. The fundamental equivalence between the G-stability and A-stability of LMMs and one-leg methods was established in 1978 [12]. Moreover, Butcher [3] studied the contractivity for Runge–Kutta methods and introduced the concept of the B-stability; see the monograph [20] for more details.

Another type of ODE systems that are very close to the contractive ODEs is the so-called dissipative systems. The main feature of the dissipative systems is the presence of certain mechanisms of energy dissipation, which can lead to quite complicated limit regimes and structures [21]. For the ODEs (1.2), Humphries and Stuart [23] imposed a structural condition on f, namely,

$$\langle f(t,x),\ x \rangle \le a - b\|x\|^2 \quad \text{for all } x \in \mathbb{R}^d \tag{1.5}$$

for some $a \ge 0$ and $b > 0$, which leads to the decay estimate of the form

$$\|x(t)\|^2 \le \|x_0\|^2 e^{-2b(t-t_0)} + \frac{a}{b}\left(1 - e^{-2b(t-t_0)}\right). \tag{1.6}$$

Hence the open ball $B(0, \sqrt{a/b} + \varepsilon)$ is an absorbing set as $t \to +\infty$ for any given $\varepsilon > 0$ and any given initial data. As defined in [23], an ODEs system is said to be dissipative if for any initial value x_0, there exists a time $t^*(x_0) \ge t_0$ and a bounded absorbing set B such that $x(t) \in B$ for all $t > t^*$[4]. We can easily see the exponential stability of $x(t)$ directly from (1.6) for $a = 0, b > 0$.

There are various models of dissipative differential equations from physics and engineering; see [21, 42]. In 1994, Humphries and Stuart [23] first studied the numerical dissipativity for Runge–Kutta methods. They proved that for DJ-irreducible Runge–Kutta methods, the algebraic stability is sufficient to imply the dissipativity of the numerical solutions to (1.2) with the dissipative condition (1.5). Based on Dahlquist's G-stability theory [12], Hill [22] demonstrated that the A-stability is equivalent to the dissipativity of LMMs and one-leg methods for ODEs with the condition (1.5).

It is very interesting and natural for us to understand if the fundamental results we have reviewed above about contractivity and dissipativity of the classical ODEs (1.2) can be established also for F-ODEs. To continue our discussions, we recall two important functions, namely the Mittag-Leffler function $E_\alpha(z)$ and the generalized Mittag-Leffler function $E_{\alpha,\beta}(z)$ defined for $z \in \mathbb{C}$:

$$E_\alpha(z) = \sum_{k=0}^{\infty} \frac{z^k}{\Gamma(\alpha k + 1)},\ \alpha > 0; \quad E_{\alpha,\beta}(z) = \sum_{k=0}^{\infty} \frac{z^k}{\Gamma(\alpha k + \beta)},\ \alpha, \beta > 0.$$

It is similar to the exponential functions that are used often in the investigation of differential equations of integer order, Mittag-Leffler type functions can be seen as the fractional generalization of exponential functions and used naturally in fractional calculus. For $\alpha \in (0,1)$, these two functions have the following nice properties [28, 40]:

$$E_\alpha(t) = E_{\alpha,1}(t) > 0,\ \ E_{\alpha,\alpha}(t) > 0,\ \ \frac{\mathrm{d}}{\mathrm{d}t}E_{\alpha,\alpha}(t) > 0, \tag{1.7}$$

the asymptotic expansion

$$E_{\alpha,\beta}(\lambda t) = -\sum_{k=1}^{N} \frac{1}{\Gamma(\beta - k\alpha)} \frac{1}{(\lambda t)^k} + O\left(\frac{1}{(\lambda t)^{N+1}}\right),\ \ N \in \mathbb{N}^+,\ \lambda < 0,\ t \to +\infty,$$

---

[4]As noted in [23], a numerical method preserves the contractivity in (1.4) is sometimes referred to be dissipative in the numerical literature, but this conflicts with the corresponding terminology in dynamical systems. At the same time, the authors in [23] give an accurate definition of dissipativity for ODEs, which mainly emphasizes the existence of a global attracting set. This definition was later widely accepted in the numerical literature, and we also follow this definition.

and the integral representation

$$\int_0^t \frac{1}{(t-\tau)^{1-\alpha}} E_{\alpha,\alpha}(\lambda(t-\tau)^\alpha)\mathrm{d}\tau = t^\alpha E_{\alpha,1+\alpha}(\lambda t^\alpha), \quad \lambda < 0, \, t > 0.$$

We first studied the Caputo F-ODEs in [43] and established the contractivity and dissipativity under the same conditions as those for classical ODEs. More precisely, we obtained the following results [43].

Lemma 1.1. (i) *Under the one-sided Lipschitz condition* (1.3) *on* f, *it holds for any two solutions* $x(t)$ *and* $y(t)$ *to the F-ODEs* (1.1) *with two initial values* x_0 *and* y_0 *that*

$$\|x(t) - y(t)\|^2 \le \|x_0 - y_0\|^2 \cdot E_\alpha(2\lambda t^\alpha). \tag{1.8}$$

In particular, we have that $\|x(t) - y(t)\| \le \|x_0 - y_0\|$ *for* $\lambda \le 0$.

(ii) *Let* $x(t)$ *be the solution of the F-ODEs* (1.1) *and* f *satisfy the dissipative condition* (1.5), *then the fractional order system is dissipative in the sense that*

$$\|x(t)\|^2 \le \|x_0\|^2 E_\alpha\left[(-2b)t^\alpha\right] + 2a \int_0^t \frac{1}{(t-\tau)^{1-\alpha}} E_{\alpha,\alpha}[(-2b)(t-\tau)^\alpha]\mathrm{d}\tau. \tag{1.9}$$

Clearly, for any given $\varepsilon > 0$, *the ball* $B(0, \sqrt{a/b} + \varepsilon)$ *is an absorbing set as* $t \to +\infty$.

We can obtain an explicit contractivity and dissipativity rates from (1.8) and (1.9) by the asymptotic expansion and integral representation of Mittag-Leffler type functions, namely, it holds for some $c_\alpha > 0$,

$$\|x(t) - y(t)\|^2 \le \|x_0 - y_0\|^2 \cdot \frac{c_\alpha}{t^\alpha}, \text{ as } t \to +\infty, \tag{1.10}$$

$$\|x(t)\|^2 \le \|x_0\|^2 \cdot \frac{c_\alpha}{t^\alpha} + \frac{a}{b}, \text{ as } t \to +\infty. \tag{1.11}$$

Here and in the rest of this work, we use c_α to represent a generic positive constant, which may take different values at different occasions, depending on α but independent of time t or discrete time points n.

We may readily observe from (1.4), (1.6), (1.10) and (1.11) that the contractivity and dissipativity rates with regard to initial values are exponential for ODEs while they are algebraic for F-ODEs. This reflects an essential difference between the long-term decay rates of solutions to classical initial value problems and fractional ones, mainly due to the nonlocal nature of fractional derivatives in some sense.

In another recent work [44], we further studied the long-time stability of the solutions to stiff nonlinear fractional functional differential equations (F-FDEs) by means of a novel fractional delay-dependent Halanary-type inequality. We investigated in [44] the effects of various functional terms such as time delay and delay integro-differential terms on the long-term properties of solutions. A variety of complex dynamic behaviors were observed for the solutions to F-FDEs due to the involvement of functional terms and fractional derivatives. In particular, we demonstrated rigorously the accurate algebraic decay rate the solutions observe with respect to various complex function perturbations in a given initial range.

When considering numerical methods for F-ODEs or F-DDEs, it is desirable that the numerical solutions can inherit the long time behavior of the solutions to original continuous equations. This motivates one of the main focuses of this paper, namely, to study the contractivity and dissipativity of solutions to the numerical F-BDFs for nonlinear F-ODEs. As we shall demonstrate both analytically and numerically, it is quite remarkable that the numerical solutions preserve exactly the same algebraic contractivity and dissipativity rates as the ones their continuous counterparts possess, described in (1.10) and (1.11).

We like to emphasize that contractivity and dissipativity for time fractional evolution equations have stronger decay behavior than the usual stability. Contractivity and dissipativity preserving numerical methods are more effective and desired in applications than those stable schemes without such long-time characteristics, especially

when the solutions have various discontinuous points. Based on the two important lemmas established in this paper, we constructed in [44] two effective difference schemes for F-FDEs, and proved that their numerical solutions preserve exactly the same algebraic contractivity rate as the one the continuous solutions observe.

To the best of our knowledge, the existing numerical stability analysis of F-ODEs is mostly focused on linear problems [8, 16–18, 35], or nonlinear problems based on the classical Lipschitz hypothesis [6, 27]. In particular, Cao *et al.* proposed the time splitting schemes in [6] and implicit-explicit difference schemes in [7] to deal with stiff nonlinear F-ODEs. The methods in [6, 7] have good linear stability without nonlinear iterations, but the special structures of the nonlinear function f were not discussed. Noting that the nonlinear F-ODEs (1.1) can be written equivalently as the Abel–Volterra integral equations of second kind with weakly singular kernel, the long time behavior was studied in [15, 38] for the numerical solutions of the corresponding integral equations. The error estimates were also obtained in [15, 38], under some stronger conditions on the function f, requiring simultaneously the monotone condition and the global Lipschitz condition. For another type of linear evolutionary Volterra integrodifferential equations in a Hilbert space H arising from the linear viscoelasticity problem, uniform behavior of some numerical methods were derived in $l_t^1(0, \infty; H) \cap l_t^\infty(0, \infty; H)$ in [46, 47] and the references therein. We note that these stability results were established in the sense of the entire time averaging, so both the results and their analyses are significantly different from the pointwise stability results and the analyses we shall develop in this work.

The rest of the paper is organized as follows. In Section 2, the contractivity rate obtained in [43] is improved for scalar F-ODEs based on nonnegative preserving properties of the solution. This result is then used to establish optimal numerical contractivity rate of F-BDFs for scalar F-ODEs in Section 3.3. In Section 3, the contractivity and dissipativity of the numerical solutions to F-BDFs are established. In Section 3.1, a discrete version of the fractional generalization of the Leibniz rule is first obtained, which allows us to derive an energy-type inequality. Then a new asymptotical behavior is studied for the solution to a linear Volterra difference equation with algebraic decay rate, which leads to the long time algebraic decay rate of the solutions to F-BDFs. The main results is proved in Section 3.2, and two typical examples of F-BDFs based on Grünwald–Letnikov and L1 difference schemes are presented in Section 3.4. The contractivity and dissipativity of some high order numerical schemes are developed in Section 3.5, under slightly stronger conditions. Several numerical examples and the concluding remarks are provided in Sections 4 and 5, respectively.

2. IMPROVED CONTRACTIVITY RATE OF SOLUTIONS TO SCALAR F-ODES

In this section, we first derive a new contractivity rate of the solutions to the scalar F-ODE:

$$_0^C D_t^\alpha x(t) = f(x(t)), \quad t > 0, \ x \in \mathbb{R}, \tag{2.1}$$

under the one-sided Lipschitz condition (1.5). This improves the main results in [43] and can be applied directly to establish optimal contractivity rate of numerical solutions to (2.1) in Section 3.3, and to the spatial semi-discrete model of linear fractional sub-diffusion equation in Section 4. The main tool in the analysis is the nonnegative preserving properties of the solutions to F-ODEs under appropriate conditions.

If the F-ODEs (1.1) is linear and stable, *i.e.*, $f(x) = Ax$, where A is a constant coefficient matrix, then we know the contractivity rate $\|x(t) - y(t)\| = O(t^{-\alpha})$ from the basic stability theory [37]. But the rate was shown to become slower for general nonlinear F-ODEs [43], namely, $\|x(t) - y(t)\| = O(t^{-\alpha/2})$; see (1.10). The energy analysis was used in [43] to estimate the decay rate of $\|x(t) - y(t)\|^2$, which is bounded by $E_\alpha(2\lambda t^\alpha)$. However, we do not have $\sqrt{E_\alpha(2\lambda t^\alpha)} = E_\alpha(\lambda t^\alpha)$ for the Mittag-Leffler function, unlike the identity $\sqrt{e^{2\lambda t}} = e^{\lambda t}$ for the classical exponential function. This is the main reason that causes the slower decay rate by the analysis in [43].

We now make use of a new analytical tool to improve the above result to the optimal contractivity rate, namely, $\|x(t) - y(t)\| = O(t^{-\alpha})$ for nonlinear scalar F-ODE. The basic idea is to estimate the decay rate of $\|x(t) - y(t)\|$ directly, not $\|x(t) - y(t)\|^2$ as it did in [43]. This enables us to avoid the square-root operation of the Mittag-Leffler function. To do this, we first present two auxiliary results.

Lemma 2.1 ([25]). *For any $x \in C[0, T] \cap C^1(0, T]$, if x takes its minimum at $t_1 \in (0, T]$, then ${}^C_0 D^\alpha_t x(t_1) \leq 0$.*

Lemma 2.2. (i) *Under the dissipation condition (1.5) with $a = 0$, if x is a solution to the equation (2.1) and $x \in C[0, +\infty) \cap C^1(0, +\infty)$, then a positive initial value $x(0)$ implies $x(t) \geq 0$ for all $t > 0$.*

(ii) *Under the one-sided Lipschitz condition (1.3) on f for some $\lambda < 0$, if x and y are two solutions to the equation (2.1) such that $x, y \in C[0, +\infty) \cap C^1(0, +\infty)$ and $x(0) > y(0)$, then $x(t) \geq y(t)$ for all $t > 0$.*

Proof. We prove by contradiction. Assume there exists a time $t_1 \in (0, T]$ for some $T > 0$ such that $x(t_1) < 0$. Then we can find a time $t_2 \in (0, T]$ such that $x(t_2) = \min_{t \in (0, T]} x(t) < 0$, hence we know ${}^C_0 D^\alpha_t x(t_2) \leq 0$ from Lemma 2.1. Using this result, we derive

$$0 \leq \big\langle {}^C_0 D^\alpha_t x(t_2), x(t_2) \big\rangle = \langle f(x(t_2)), x(t_2) \rangle \leq \lambda \|x(t_2)\|^2 < 0. \tag{2.2}$$

This contradiction yields the desired result in (i). The result in (ii) can be proved by the same argument. $\square$

Theorem 2.3. *Under the same conditions on f, x and y as in Lemma 2.2(ii) except that $x(0)$ may not be bigger than $y(0)$, the following asymptotic estimate holds*

$$\|x(t) - y(t)\| \leq \|x_0 - y_0\| \cdot \frac{c_\alpha}{t^\alpha} \quad as \ t \to +\infty. \tag{2.3}$$

Proof. Let $z(t) = x(t) - y(t)$, and we assume $z(0) > 0$ (the same argument for $z(0) < 0$). We readily see $z(t) \geq 0$ for all $t > 0$ from Lemma 2.2, and

$$\big\langle {}^C_0 D^\alpha_t z(t), z(t) \big\rangle = \langle f(x(t)) - f(y(t)), z(t) \rangle \leq \lambda \|z(t)\|^2 < 0 \tag{2.4}$$

due to the one-sided Lipschitz condition.

It follows from (2.4) that $z(t) \cdot {}^C_0 D^\alpha_t z(t) \leq \lambda \|z(t)\|^2 = \lambda \, (z(t))^2$, which yields that ${}^C_0 D^\alpha_t z(t) \leq \lambda z(t)$, by noting the fact that $z(t) \geq 0$ and is scalar. This inequality implies directly $z(t) \leq z(0) E_\alpha(\lambda t^\alpha)$. Now the desired estimate follows from the asymptotic expansion of the Mittag-Leffler function. $\square$

By a similar argument to the one of Theorem 2.3 above, we can show that the dissipativity rate in (1.11) for the solution $x(t)$ to the scalar F-ODE (2.1) can be improved:

$$\|x(t)\| \leq \|x_0\| \cdot \frac{c_\alpha}{t^\alpha} \quad as \ t \to +\infty, \tag{2.5}$$

under the dissipativity condition (1.5) with $a = 0$ and $b > 0$.

For a general nonlinear system (1.1) with $d > 1$, we cannot expect the same contractivity rate as the one (*cf.* (2.3)) for the linear systems or the nonlinear scalar equation. We guess that the contractivity rate obtained in (1.10) should be optimal for the nonlinear systems that can not be decoupled by diagonalization (note that the rate in (1.10) is only the half of the rate shown in (2.3)), and this is confirmed in Section 4 by numerical experiments. We can easily see that a similar derivation as we did for (2.3) above from the inequality (2.4) does not apply for the general nonlinear system (1.1) with $d > 1$. That is, we can not get ${}^C_0 D^\alpha_t \|z(t)\| \leq \lambda \|z(t)\|$ in general from the inequality $z(t)^T \cdot {}^C_0 D^\alpha_t z(t) \leq \lambda \|z(t)\|^2$ for the vector-valued case ($d > 1$), for which a more sophisticated functional framework may be needed.

3. Contractivity and dissipativity analysis of F-BDFs

In this section we investigate the contractivity and dissipativity of numerical solutions to F-BDFs. Let $h > 0$ be the step-size and $t_n = nh, n = 0, 1, 2, 3, \ldots$ be the corresponding time nodal points. Further, we write x_n for the approximation of $x(t_n)$ and $f_n = f(t_n, x_n)$. As in integer-order differential equations, one basic approach of constructing difference schemes is based on the numerical differentiation of fractional derivatives. Because of

the nonlocal nature of fractional derivatives, the numerical approximation involves all discrete time points from t_0 to t_n, leading to the numerical method for F-ODEs (1.1) in the following full-term recursion

$$\sum_{j=0}^{n} \omega_{n-j} x_j = h^\alpha f_n, \quad n = 1, 2, 3, \ldots. \tag{3.1}$$

There are several approaches in the literature for determining the weight coefficients $\{\omega_n\}_{n=0}^{\infty}$, which yield a wide variety of numerical methods with different accuracies and stabilities. Solutions to time fractional equations often exhibit weak singularities at the origin, resulting in slower convergence rates of numerical solutions. Correction formulas were developed in [26, 36] to restore the convergence rate. Since the correction terms do not affect the stability of numerical methods, we shall not consider them in this work.

Due to the major characteristic difference between F-ODEs and ODEs, the traditional analytical tools developed by Dahlquist [12] can not easily extended to F-ODEs. It is well known that the concept of G-stability plays a central role [12,20,22] in the study of the contractivity and dissipativity of LMMs and one-leg methods for classical ODEs, and most analyses are performed under the G-norm in $\mathbb{R}^{d \cdot k}$. Unfortunately, the G-norm can not extend to F-LMMs, mainly because of the nonlocal nature of fractional operators, for which the dimension of the G matrix increases with the time and is no longer fixed.

We consider the F-BDFs in (3.1) for F-ODEs in $\mathbb{R}^d$ with $d \geq 1$. The numerical contractivity and dissipativity with polynomial decay rate will be established under some natural assumptions on the weight coefficients $\{\omega_n\}_{n=0}^{\infty}$. It can be verified that Grünwald–Letnikov formula [40] and the L1 method [33, 41] fully satisfy our assumptions. In particular, for the scalar F-ODE with $d = 1$, the decay rate can be improved to be the optimal one (*cf.* Sect. 3.3), exactly as in the continuous case given in Section 2. We further study in Section 3.5 the numerical contractivity and dissipativity for two second order schemes for F-ODEs in $\mathbb{R}^d$ with $d \geq 1$ under some slightly stronger conditions.

We like to point out that we consider only the F-BDF like methods of the form (3.1) in this work. There are many other general numerical schemes, such as classical quadratures, collocation methods, for which the analysis could be much more complicated, and more analytical tools or refined analyses may need to be developed.

3.1. Preliminaries

In this subsection, we present some auxiliary results for the subsequent analysis. An inner product inequality involving Caputo fractional derivatives played a key role in our analysis of F-ODEs [43], and the inequality was originated from the following important equality by Alikhanov, which is a fractional variant of the classical Leibniz formula.

Lemma 3.1 ([1]). *For any two absolutely continuous functions $x(t)$ and $y(t)$ on $[0, T]$, the following equality holds for $0 < \alpha < 1$:*

$$x^T(t) \cdot {}_{0}^{C}D_t^\alpha y(t) + y^T(t) \cdot {}_{0}^{C}D_t^\alpha x(t) = {}_{0}^{C}D_t^\alpha \left(x^T(t) \cdot y(t) \right) \tag{3.2}$$

$$+ \frac{\alpha}{\Gamma(1-\alpha)} \int_0^t \frac{1}{(t-\xi)^{1-\alpha}} \left(\int_0^\xi \frac{x'(\eta)\mathrm{d}\eta}{(t-\eta)^\alpha} \cdot \int_0^\xi \frac{y'(s)\mathrm{d}s}{(t-s)^\alpha} \right) \mathrm{d}\xi.$$

We can easily derive the inequality

$${}_{0}^{C}D_t^\alpha \left(x^T(t) \cdot x(t) \right) \leq 2x^T(t) \cdot {}_{0}^{C}D_t^\alpha x(t) \quad \text{for} \ \ 0 < \alpha < 1 \tag{3.3}$$

by taking $x(t) = y(t)$ in the identity (3.2) and noting the fact that $\frac{\alpha}{\Gamma(1-\alpha)} \int_0^t \frac{\mathrm{d}\xi}{(t-\xi)^{1-\alpha}} \left(\int_0^\xi \frac{x'(\eta)\mathrm{d}\eta}{(t-\eta)^\alpha} \right)^2 \geq 0$.

We shall start with the contractivity and dissipativity of numerical solutions to F-BDF (3.1) under the following general assumptions on the weights $\{\omega_n\}_{n=0}^{\infty}$:

$$\text{Assumption } (I) : \quad \begin{cases} \text{(i)} \quad \omega_0 > 0, \\ \text{(ii)} \quad \omega_j \le 0 \text{ for all } j \ge 1, \\ \text{(iii)} \quad \sum\limits_{j=0}^{n} \omega_j \ge 0 \text{ for any given } n \ge 1, \end{cases}$$

then apply the results to two specific F-BDFs, based on Grünwald–Letnikov formula and L1 method.

As it is seen, the main motivation of Assumption (I) is for deriving the following discrete version of the inequality (3.3), which is crucial to help us establish the numerical dissipativity and contractivity of F-BDFs.

Lemma 3.2. *Under Assumption (I), it holds for the F-BDF (3.1):*

$$\sum_{j=0}^{n} \omega_{n-j} \|x_j\|^2 \le \left\langle 2x_n, \sum_{j=0}^{n} \omega_{n-j} x_j \right\rangle, \quad n \ge 1. \tag{3.4}$$

Proof. The desired result comes from the direct calculations:

$$\left\langle 2x_n, \sum_{j=0}^{n} \omega_{n-j} x_j \right\rangle - \sum_{j=0}^{n} \omega_{n-j} \|x_j\|^2 = \left\langle 2x_n, \sum_{j=0}^{n} \omega_{n-j} x_j \right\rangle - \sum_{j=0}^{n} \omega_{n-j} \|x_n\|^2 - \sum_{j=0}^{n} \omega_{n-j} \|x_j\|^2 + \sum_{j=0}^{n} \omega_j \|x_n\|^2$$

$$= \left\langle 2x_n, \sum_{j=0}^{n} \omega_{n-j} x_j \right\rangle - \sum_{j=0}^{n-1} \omega_{n-j} \|x_n\|^2 - \sum_{j=0}^{n-1} \omega_{n-j} \|x_j\|^2 + \sum_{j=0}^{n} \omega_j \|x_n\|^2$$

$$\ge -\sum_{j=0}^{n-1} \omega_{n-j} \left(\|x_n\| - \|x_j\| \right)^2 + \left(\sum_{j=0}^{n} \omega_j \right) \|x_n\|^2 \ge 0,$$

where we have used Assumption (I) on the weight coefficients in the last inequality. □

The numerical discretization of F-ODEs often leads to some Volterra difference equations of convolution type. The relevant results and analytical tools for Volterra difference equations are often employed to study the stability and asymptotic behavior of fractional numerical schemes [8]. We now introduce some important results on the boundedness and asymptotic decay rate for the solutions to a class of linear convolution Volterra difference equations.

General speaking, it is much more difficult to achieve the exact decay rates of the solutions to difference equations than to establish qualitative properties such as the stability or asymptotic stability of some equilibrium solutions. Applelby, Győri and Rennolds [2] derived exact convergence rates of some linear Volterra difference equations by making use of an elegant three-term decomposition of the discrete convolution; see Appendix A for the relevant concepts and the main results in [2]. A remarkable advantage of Lemma A.1 is that the class of kernels could decay sub-exponentially, which allows us to derive the non-exponential convergence rates for some asymptotically stable nontrivial solutions. This approach applies also to the difference schemes of F-ODEs, so we shall adopt it to derive the boundedness and exact contractivity rate of the F-BDF (3.1). For the sake of ease exposition, we shall often write in the rest of the paper that $a_n \sim b_n$ for any two sequence $\{a_n\}$ and $\{b_n\}$ that are equivalent in the sense $\lim_{n\to\infty} a_n/b_n = 1$.

Lemma 3.3. *Consider the Volterra difference equation*

$$x_{n+1} = d_n + \sum_{j=0}^{n} D_{n-j} x_j, \quad n \ge 1, \tag{3.5}$$

where the coefficients satisfy $d_n \sim \frac{c_1}{n^\alpha}$, $D_n \sim \frac{c_2}{n^{1+\alpha}}$, *and* $\rho = \sum_{j=0}^\infty |D_j| < 1$, *for some constants* $c_1, c_2 > 0$ *and* $0 < \alpha < 1$. *Then we have the asymptotic estimate* $x_n \sim \frac{c_1(1-\rho)^{-1}}{n^\alpha}$.

Proof. We apply Lemma A.1 for the desired result, but we can not apply Lemma A.1 directly as the conditions there are not satisfied, namely $d_n \sim c_1/n^\alpha$ and $\widetilde{\gamma}_n = 1/(n+1)^\alpha \notin W(1)$ for $0 < \alpha < 1$ (see the exact definition of $W(1)$ in Appendix A), and that the series $\sum_{j=1}^\infty 1/n^\alpha$ diverges.

Instead, we transform the equation (3.5) to a different one for which Lemma A.1 is applicable. To do so, we introduce a simple transformation $y_n = \frac{x_n}{n}$ for $n \geq 1$, and let $y_0 = x_0$, $g_n = \frac{d_n}{n+1}$ and $G_{n,j} = \frac{j}{n+1}D_{n-j}$. Then the equation (3.5) becomes

$$y_{n+1} = g_n + \sum_{j=0}^n G_{n,j} \, y_j, \quad n \geq 1. \tag{3.6}$$

We may note that (3.5) is a convolution difference equation while equation (3.6) is not. Obviously, it holds that $g_n \to c_1/n^{1+\alpha}$ as $n \to \infty$. Following the idea developed in [2], we now take the weight sequence $\gamma_n = 1/(n+1)^{1+\alpha} \in W(1)$ and compute $L_\gamma(y) = \lim_{n\to\infty} y_n/\gamma_n$ to give a non-trivial limit, which yields that y_n behaves like $O(n^{-(1+\alpha)})$ asymptotically. Letting $z_n = y_n/\gamma_n$, we can rewrite equation (3.6) as

$$z_{n+1} = h_n + \sum_{j=0}^n H_{n,i} \, z_j, \quad n \geq 1, \tag{3.7}$$

with $h_n = \frac{g_n}{\gamma_{n+1}}$, $H_{n,j} = \frac{\gamma_j}{\gamma_{n+1}}G_{n,j} = \frac{j}{n+1}\frac{\gamma_j}{\gamma_{n+1}}D_{n-j}$. Now we plan to derive the limit of z_n satisfying equation (3.7) by Lemma A.1. It suffices to verify all the conditions in the lemma. Firstly, it is easy to see

$$\lim_{n\to\infty} \sup_{n\geq 0} \sum_{j=0}^m |H_{n,n-j}| = \sum_{j=0}^m |D_j| \lim_{n\to\infty}\left(\frac{n-j}{n+1}\frac{\gamma_{n-j}}{\gamma_{n+1}}\right) = \sum_{j=0}^m |D_j|,$$

therefore, $\lim_{m\to\infty} \sup_{m\geq 0}\left(\lim_{n\to\infty}\sup_{n\geq 0}\sum_{j=0}^m |H_{n,n-j}|\right) = \sum_{j=0}^\infty |D_j| = \rho < 1$. Secondly, for any fixed $m > 0$, we have

$$\lim_{n\to\infty}\sup_{n\geq 0}\sum_{j=m}^{n-m} |H_{n,n-j}| \leq \sup_{l\geq m}\left(\frac{|D_l|}{\gamma_l}\right)\lim_{n\to\infty}\frac{\gamma_n}{\gamma_{n+1}}\lim_{n\to\infty}\sup_{n\geq 0}\left(\sum_{j=m}^{n-m}\frac{n-j}{n+1}\frac{\gamma_{n-j}\gamma_j}{\gamma_n}\right).$$

This implies that $\lim_{m\to\infty}\left(\lim_{n\to\infty}\sup_{n\geq 0}\sum_{j=m}^{n-m} |H_{n,n-j}|\right) = 0$ by noting that $\lim_{m\to\infty}\left(\lim_{n\to\infty}\sup_{n\geq 0}\sum_{j=m}^{n-m}\frac{\gamma_{n-j}\gamma_j}{\gamma_n}\right) = 0$; see Appendix A. It remains to compute that

$$\lim_{n\to\infty} H_{n,m} = \lim_{n\to\infty}\left(\frac{m}{n+1}\frac{\gamma_{n-m}}{\gamma_{n+1}}\frac{D_{n-m}}{\gamma_{n-m}}\right)\gamma_m,$$

which implies that $H_{\infty,m} = \lim_{n\to\infty} H_{n,m} = 0$. In fact, it follows directly from Lemma A.1 that $\lim_{n\to\infty} z_n = L_\gamma(y) = (1-\rho)^{-1} L_\gamma(g)$, which leads readily to our desired estimate

$$y_n = \frac{x_n}{n} \sim \frac{c_1(1-\rho)^{-1}}{n^{1+\alpha}},$$

and competes the proof. $\qquad\square$

The discrete energy inequality in Lemma 3.2 and the $O(n^{-\alpha})$ decay rate of Volterra difference equation in Lemma 3.3 are crucial in our subsequent analysis. They are also very useful for analyzing the long-term stability and decay rate of other more complex problems, such as F-FDEs [44] and time fractional PDEs.

Although we consider only the uniform grids in this work, we hope that our analytical techniques may provide some meaningful insights for non-uniform grid methods, especially for the popular graded grids and the non-uniform L1 formula [29], which are very useful when we construct adaptive numerical methods or schemes with relatively large time steps.

3.2. Numerical contractivity and dissipativity

We now present one of our main results in this paper, which can be seen as the discrete version of Lemma 1.1.

Theorem 3.4. *Assume that the weights $\{\omega_k\}_{n=0}^{\infty}$ of the F-BDF (3.1) satisfy Assumption (I), and there exists a constant $c_{\alpha} > 0$ such that for any given $n \geq 2$, $|\omega_k| \leq c_{\alpha}/k^{1+\alpha}$ for $1 \leq k \leq n-1$ and $|\omega_n| \leq c_{\alpha}/n^{\alpha}$.*

(i) *If function f in (3.1) satisfies the one-sided Lipschitz condition (1.3), and $\rho_1 = \lim_{n\to\infty} \sum_{j=1}^{n} \frac{|\omega_j|}{\omega_0 - 2\lambda h^{\alpha}} < 1$ for any $h > 0$, then the F-BDF (3.1) is contractive, and its solution can preserve the exact contractivity rate as the true solution to F-ODEs (1.1) (cf. (1.10)), namely, $\|x_n - y_n\|^2 \leq c_1 \|x_0 - y_0\|^2 n^{-\alpha}$ as $n \to \infty$, with $c_1 = (1 - \rho_1)^{-1} \frac{c_{\alpha}}{\omega_0 - 2\lambda h^{\alpha}}$.*

(ii) *If function f in (3.1) satisfies condition (1.5), and $\rho_2 = \lim_{n\to\infty} \sum_{j=1}^{n} \frac{|\omega_j|}{\omega_0 + 2bh^{\alpha}} < 1$ for any $h > 0$, then the F-BDF is dissipative, i.e., for any given initial value x_0 and $\varepsilon > 0$, there is a bounded set $B(0, r)$ and $n_0 \in N^+$ such that $x_n \in B(0, r)$ for all $n \geq n_0$, with $r = \sqrt{c_2 a/b} + \varepsilon$ and $c_2 = (1 - \rho_2)^{-1}$. Moreover, if the condition (1.5) is satisfied with $a = 0$, the numerical solution has the exact dissipativity rate as the exact solution to F-ODEs (1.1), namely, $\|x_n\|^2 \leq c_3 \|x_0\|^2 n^{-\alpha}$ as $n \to \infty$, with $c_3 = (1 - \rho_2)^{-1} \frac{c_{\alpha}}{\omega_0 + 2bh^{\alpha}}$.*

Proof. (i) Let x_j and y_j be the numerical solutions of the F-BDF (3.1) with two different initial values x_0 and y_0, respectively. Put $z_n = x_n - y_n, n \geq 0$. We can easily see that $\sum_{j=0}^{n} \omega_{n-j} z_j = h^{\alpha} (f(x_n) - f(y_n))$. Taking the inner product with $2z_n$ on both sides and applying the one-sided Lipschitz condition and Lemma 3.2, we get

$$\sum_{j=0}^{n} \omega_{n-j} \|z_j\|^2 \leq 2\lambda h^{\alpha} \|z_n\|^2, \tag{3.8}$$

which can be rewritten as $(\omega_0 - 2\lambda h^{\alpha}) \|z_n\|^2 \leq \sum_{j=0}^{n-1} |\omega_{n-j}| \|z_j\|^2$ by noting that $\omega_{n-j} < 0$ for $j = 0, 1, \ldots, n-1$. Since the weights ω_n and ω_j for $j \leq n-1$ have different decay rates, the above Volterra difference inequality can be further rewritten as

$$\|z_n\|^2 \leq \frac{|\omega_n|}{\omega_0 - 2\lambda h^{\alpha}} \|z_0\|^2 + \sum_{j=1}^{n-1} \frac{|\omega_{n-j}|}{\omega_0 - 2\lambda h^{\alpha}} \|z_j\|^2, \quad n \geq 2.$$

Now applying Lemma 3.3 yields the desired decay rate $\|z_n\|^2 \leq (1 - \rho_1)^{-1} \frac{\|z_0\|^2}{\omega_0 - 2\lambda h^{\alpha}} \frac{c_{\alpha}}{n^{\alpha}} = c_1 \frac{\|z_0\|^2}{n^{\alpha}}$ as $n \to \infty$.

(ii) It follows directly from the dissipativity condition (1.5) and Lemma 3.2 that

$$\left\langle 2x_n, \sum_{j=0}^{n} \omega_{n-j} x_j \right\rangle = 2h^{\alpha} \langle f_n, x_n \rangle \leq 2h^{\alpha} \left(a - b\|x_n\|^2 \right),$$

which implies that $(\omega_0 + 2h^{\alpha} b) \|x_n\|^2 \leq 2h^{\alpha} a - \sum_{j=0}^{n-1} \omega_{n-j} \|x_j\|^2$ for $n \geq 1$, leading to the convolution Volterra inequality

$$\|x_n\|^2 \leq \frac{2h^{\alpha} a}{\omega_0 + 2h^{\alpha} b} + \sum_{j=0}^{n-1} \frac{|\omega_{n-j}|}{\omega_0 + 2h^{\alpha} b} \|x_j\|^2, \quad n \geq 2.$$

By applying Lemma A.1, we obtain that $\|x_n\|^2 \leq (1-\rho_2)^{-1} \frac{2h^\alpha a}{\omega_0 + 2h^\alpha b} \leq c_2 \frac{a}{b}$ as $n \to \infty$, where $\rho_2 = \lim_{n\to\infty} \sum_{j=1}^n \frac{|\omega_j|}{\omega_0 + 2h^\alpha b} < 1$ and $c_2 = (1-\rho_2)^{-1}$. The poof of the desired dissipativity rate for $a = 0, b > 0$ is similar to the proof of (i) and omitted here. $\qquad\square$

One may observe from the proof of part (ii) in Theorem 3.4, it is not easy to derive the dissipativity result by the usual Grönwall-like inequalities, because those estimates depend often directly on the initial values x_0, but the dissipativity is a long time feature of solutions to F-ODEs and is independent of the initial values.

An alternative approach for the boundedness of $\|x_n\|$ in part (ii) of Theorem 3.4 is to apply some discrete variants of a Paley–Wiener theorem, which was introduced by Lubich [35]. We demonstrate below that the results obtained by this approach is consistent to the ones in Theorem 3.4. We first recall a result from [35].

Lemma 3.5. *Consider the discrete Volterra equation $y_n = p_n + \sum_{j=0}^n q_{n-j} y_j, n \geq 1$, where the kernel $\{q_n\}_{n=0}^\infty$ belongs to l^1, i.e., $\sum_{j=0}^\infty |q_j| < \infty$. Then $y_n \to 0$ (resp. bounded) whenever $p_n \to 0$ (resp. bounded) as $n \to \infty$ if and only if the Paley–Wiener condition is satisfied, i.e.,*

$$\sum_{j=0}^\infty q_j \zeta^j \neq 1 \text{ for } |\zeta| \leq 1. \tag{3.9}$$

If we define a sequence $\{r_n\}_{n=0}^\infty$ by $\frac{1}{1-\sum_{j=0}^\infty q_j \zeta^j} = \sum_{j=0}^\infty r_j \zeta^j$, we can easily check from the proof of Lemma 3.5 that if $\{q_n\}_{n=0}^\infty$ belongs to l^1 and the Paley–Wiener condition (3.9) holds, then $\{r_n\}_{n=0}^\infty$ is also in l^1, and the estimate holds $\|y\|_{l^\infty} \leq \|r\|_{l^1} \|p\|_{l^\infty}$.

Now consider the Volterra difference equation related to (ii) of Theorem 3.4, *i.e.*,

$$\|x_n\|^2 = \frac{2h^\alpha a}{\omega_0 + 2h^\alpha b} + \sum_{j=0}^{n-1} \frac{|\omega_{n-j}|}{\omega_0 + 2h^\alpha b} \|x_j\|^2 \text{ for } n \geq 1.$$

The assumption $\rho_2 = \lim_{n\to\infty} \sum_{j=1}^n \frac{|\omega_j|}{\omega_0 + 2bh^\alpha} < 1$ implies that the kernel $\left\{\frac{|\omega_j|}{\omega_0 + 2bh^\alpha}\right\}_{j=1}^\infty$ belongs to l^1 and the corresponding Paley–Wiener condition $\sum_{j=1}^\infty \frac{|\omega_j|\zeta^j}{\omega_0 + 2bh^\alpha} \neq 1$ for $|\zeta| \leq 1$ holds. Let

$$\frac{1}{1 - \sum\limits_{j=1}^\infty \frac{|\omega_j|\zeta^j}{\omega_0 + 2bh^\alpha}} = \sum_{j=0}^\infty r_j \zeta^j \text{ for } |\zeta| \leq 1. \tag{3.10}$$

Then $r_j \geq 0$ and $\{r_n\}_{n=0}^\infty$ is in l^1. Taking $\zeta = 1$ in (3.10) yields that

$$\|x_n\|^2 \leq \|r\|_{l^1} \frac{2h^\alpha a}{\omega_0 + 2h^\alpha b} = (1-\rho_2)^{-1} \frac{2h^\alpha a}{\omega_0 + 2h^\alpha b} \leq (1-\rho_2)^{-1} \frac{a}{b} \text{ as } n \to \infty,$$

which is the same as the corressponding results in part (ii) of Theorem 3.4.

3.3. Improved numerical contractivity rates for scalar F-ODEs

In Section 2, we presented an optimal contractivity rate for the scalar F-ODE (2.1). A typical application of this new result is for the spatial semi-discrete model of linear fractional sub-diffusion equation, and this will be carefully validated by numerical experiments in Section 4. Next we demonstrate that this optimal contractivity rate can be preserved exactly by the numerical solutions to the scalar F-ODE (2.1). We first derive some nonnegative preserving properties of the numerical solutions to the F-BDF (3.1) for (2.1).

Lemma 3.6. *Let function f in the scalar F-ODE (2.1) satisfy that $\langle f(x), x \rangle \leq \lambda \|x\|^2$ for some $\lambda < 0$, and $x(t)$ be the solution to (2.1) with $x(0) > 0$. Then under Assumption (I), the solutions to the F-BDF (3.1) are all nonnegative.*

Proof. We prove by mathematical induction. For $n = 1$, we see directly from (3.1) that $\omega_1 x_0 + \omega_0 x_1 = h^\alpha f(x_1)$. Then we can get by taking the inner product with x_1 on both sides that $-\omega_1 x_0 x_1 \geq (\omega_0 - h^\alpha \lambda) x_1^2 \geq 0$, which implies $x_1 \geq 0$.

We now prove $x_n \geq 0$ under the condition that $x_j \geq 0$ for $j = 1, 2, \ldots, n-1$. Taking the inner product with x_n in both sides of the F-BDF (3.1) gives that $\langle x_n, \sum_{j=0}^n \omega_{n-j} x_j \rangle = h^\alpha \langle f_n, x_n \rangle \leq h^\alpha \lambda \|x_n\|^2$, which can be rewritten as

$$x_n \left(-\sum_{j=0}^{n-1} \omega_{n-j} x_j \right) \geq (\omega_0 - h^\alpha \lambda) \|x_n\|^2 \geq 0.$$

This implies that $x_n \geq 0$. $\qquad\square$

Theorem 3.7. *Let function f in the scalar F-ODE (2.1) satisfy the one-sided Lipschitz condition (1.3), x_n and y_n are two solutions to the F-BDF (3.1) with different initial values x_0 and y_0. Then under Assumption (I), the following contractivity estimate holds*

$$\|x_n - y_n\| \leq \|x_0 - y_0\| \cdot \frac{c_1}{n^\alpha}, \ \ as \ n \to \infty, \tag{3.11}$$

where c_1 is the same as in Theorem 3.4.

On the other hand, if function f in the scalar F-ODE (2.1) satisfies the dissipative condition (1.5) with $a = 0$, then the solutions to the F-BDF (3.1) decay as

$$\|x_n\| \leq \|x_0\| \cdot \frac{c_3}{n^\alpha} \ \ as \ n \to \infty \ \ (c_3 \ is \ the \ same \ as \ in \ Thm. \ 3.4). \tag{3.12}$$

Proof. The proof is very similar to the one of Theorem 3.4, but we estimate the decay rate of $z_n = x_n - y_n$ directly rather than $\|x_n - y_n\|^2$, which allows us to avoid the square-root operation of the Mittag-Leffler function. Without lose of generality, we assume $z_0 = x_0 - y_0 > 0$. Using the dissipative condition (1.5), we can derive

$$\left\langle z_n, \sum_{j=0}^n \omega_{n-j} z_j \right\rangle = h^\alpha \langle z_n, f(x_n) - f(y_n) \rangle \leq h^\alpha \lambda \|z_n\|^2, \tag{3.13}$$

then it follows from Lemma 3.6 that $z_n \geq 0$ for all $n \geq 1$. This non-negativity and the inequality (3.13) yield that $\sum_{j=0}^n \omega_{n-j} z_j \leq h^\alpha \lambda \|z_n\| = h^\alpha \lambda z_n$, from which and Lemma 3.3 the contractivity rate (3.11) follows readily. The proof of the dissipativity rate (3.12) can be done similarly. $\qquad\square$

3.4. Examples of F-BDFs

In this subsecion, we present some concrete examples of F-BDFs, whose weights $\{\omega_j\}_{j=0}^\infty$ meet all the conditions required for the results we have derived in the previous three subsections. We consider two widely used low-order schemes of the form F-BDF (3.1), *i.e.*, the Grünwald–Letnikov formula [40] and the L1 method [33,41]. The coefficients of these two schemes carry very nice properties that enable us to establish the energy-type inequality in Lemma 3.2 and the decay rate in Lemma 3.3 directly.

3.4.1. Grünwald–Letnikov formula

The approximate formula of the Grünwald–Letnikov (G–L) fractional derivative [28,40] can be given by

$$_0^{GL}D_t^\alpha x(t_n) = \frac{1}{h^\alpha} \sum_{k=0}^n (-1)^k \binom{\alpha}{k} x_{n-k} + O(h) = \frac{1}{h^\alpha} \sum_{k=0}^n \omega_k x_{n-k} + O(h) \tag{3.14}$$

for $0 < \alpha < 1$, where the coefficients are given by $\omega_k = (-1)^k \begin{pmatrix} \alpha \\ k \end{pmatrix}$, $k = 0, 1, \ldots, n$, while the Caputo derivative can be described by

$$
{}_0^C D_t^\alpha x(t_n) = \frac{1}{h^\alpha} \left(\sum_{j=1}^n \omega_{n-j} x_j + \delta_n x_0 \right) + O(h), \tag{3.15}
$$

where the coefficient δ_n is set to be $\delta_n = -\sum_{j=0}^{n-1} \omega_j$ so that the sum of the weights in (3.15) equals to zero, which is beneficial to the numerical stability of the scheme [16]. The G–L formula is a simple and effective numerical scheme with first order accuracy, and its weights ω_k meet the following properties.

Lemma 3.8 ([16]). *For $0 < \alpha < 1$, the coefficients $\omega_k = (-1)^k \begin{pmatrix} \alpha \\ k \end{pmatrix}$ satisfy*

(i) $\omega_0 = 1$, $\omega_n < 0, |\omega_{n+1}| < |\omega_n|$, $n = 1, 2, \ldots$;

(ii) $\omega_0 = -\sum_{j=1}^\infty \omega_j > -\sum_{j=1}^n \omega_j$, $n \geq 1$;

(iii) $\omega_n = O(n^{-1-\alpha})$, $\delta_n = O(n^{-\alpha})$ as $n \to \infty$.

3.4.2. L1 method

The L1 method is among the most popular algorithms for the discretization of the Caputo derivative. It often leads to unconditionally stable algorithms, and has the accuracy $O(h^{2-\alpha})$ for smooth data [33,41] and the order $O(h)$ for non-smooth data in uniform grids [24]. The L1 method can be written as

$$
{}_0^C D_t^\alpha x(t)|_{t=t_n} = \frac{1}{h^\alpha} \sum_{k=0}^{n-1} b_{n-k-1} (x_{k+1} - x_k) + O(h^q) = \frac{1}{h^\alpha} \sum_{k=0}^n \gamma_{n-k} x_k + O(h^q), \tag{3.16}
$$

where $O(h^q)$ is the local truncation error with order $q = 1$ or $2 - \alpha$, and the weight coefficients are given by $b_k = \frac{1}{\Gamma(2-\alpha)} \left((k+1)^{1-\alpha} - k^{1-\alpha} \right)$ for $0 \leq k \leq n-1$, $\gamma_0 = \frac{1}{\Gamma(2-\alpha)}$, $\gamma_k = \frac{1}{\Gamma(2-\alpha)} \left((k+1)^{1-\alpha} - 2k^{1-\alpha} + (k-1)^{1-\alpha} \right)$ for $k = 1, 2, \ldots, n-1$, and $\gamma_n = \frac{1}{\Gamma(2-\alpha)} \left((n-1)^{1-\alpha} - n^{1-\alpha} \right)$. The second formula in (3.16) is the discrete convolution quadrature and its coefficients have the following properties, which can be checked directly.

Lemma 3.9. *The coefficients of the L1 method meet the properties:*

(i) $\gamma_0 > 0, \gamma_1 < \gamma_2 < \ldots < \gamma_{n-1} < 0$, $\gamma_n < 0$ *for any* $n \geq 1$;

(ii) $\gamma_k \sim -\dfrac{\alpha}{\Gamma(1-\alpha)k^{1+\alpha}}$ *as* $k \to \infty$ *for $k \neq n$, and* $\gamma_n \sim -\dfrac{1}{\Gamma(1-\alpha)n^\alpha}$ *as* $n \to \infty$.

A common feature of the G–L formula and L1 method is that the sign of the weights $\{\omega_j\}_{j \geq 1}$ and $\{\gamma_j\}_{j \geq 1}$ remain negative, which are crucial to the results in Lemma 3.2. But this feature is no long true for high order schemes, such as the fractional trapezoidal rule, the second order F-BDF formula and fractional Newton-Gregory formula, and there are always some positive weights [18]. Another important feature of the G–L formula and L1 method is that their weights δ_n and γ_n decay in the order $O(n^{-\alpha})$. But the coefficients of the schemes for the F-ODEs with the Riemann–Liouville fractional derivative decay faster, namely, in the order $O(n^{-1-\alpha})$. We emphasize that the decay rates of the weights δ_n and γ_n essentially determine the decay rates of the numerical method (3.1); see Lemma 3.3.

For both the G–L formula and L1 method, we now verify the conditions in Theorem 3.4 are satisfied. Indeed, for the G–L formula, we have

$$
\rho_1 = \lim_{n \to \infty} \sum_{j=1}^n \frac{|\omega_j|}{\omega_0 - 2\lambda h^\alpha} = \frac{1}{1 - 2\lambda h^\alpha} < 1, \quad c_1 = \left(1 - \frac{1}{2\lambda h^\alpha} \right) \frac{c_\alpha}{1 - 2\lambda h^\alpha},
$$

$$
\rho_2 = \lim_{n \to \infty} \sum_{j=1}^n \frac{|\omega_j|}{\omega_0 + 2bh^\alpha} = \frac{1}{1 + 2bh^\alpha} < 1, \quad c_2 = 1 + \frac{1}{2bh^\alpha},
$$

while for the L1 method, we have

$$\rho_1 = \frac{1}{1 - 2\Gamma(2-\alpha)\lambda h^\alpha} < 1, \ c_1 = \left(1 - \frac{1}{2\Gamma(2-\alpha)\lambda h^\alpha}\right) \frac{c_\alpha}{1 - 2\Gamma(2-\alpha)\lambda h^\alpha},$$

$$\rho_2 = \frac{1}{1 + 2\Gamma(2-\alpha)bh^\alpha} < 1, \ c_2 = 1 + \frac{1}{2b\Gamma(2-\alpha)h^\alpha}.$$

The above shows both methods satisfy all the conditions of Theorem 3.4, therefore are contractive, dissipative, and preserve the optimal contractivity rate.

3.5. High order numerical approximations

In this subsection, we establish the contractivity and dissipativity of the F-BDFs for some high order approximations under slightly stronger conditions than those in (1.3) and (1.5). As two typical examples, we consider the convolution quadrature schemes based on classical second order BDF [10,18,36] and the product integration schemes based on quadratic interpolation approximation [19,34].

3.5.1. Second order F-BDFs

Second order F-BDFs have good stability as the first order G–L formula, but with higher accuracy. Due to the weak singularity of the solutions of time fractional order equations at the initial time, special correction techniques are usually needed to restore the full order at the initial steps [10,26]. The numerical method in (3.1) can be written

$$_0^C D_t^\alpha x(t_n) = \frac{1}{h^\alpha}\left(\sum_{j=1}^n \mu_{n-j}x_j + \delta_n x_0\right) + O(h^q),$$

where the coefficient δ_n is given by $\delta_n = -\sum_{j=0}^{n-1}\mu_j$, while the weights $\{\mu_j\}$ are generated by the function

$$\mu(\xi) = \left(\frac{3}{2} - 2\xi + \frac{1}{2}\xi^2\right)^\alpha = \left(\frac{3}{2}\right)^\alpha (1-\xi)^\alpha \left(1 - \frac{1}{3}\xi\right)^\alpha = \sum_{n=0}^\infty \mu_j\xi^j, \tag{3.17}$$

and can be computed by $\mu_j = \left(\frac{3}{2}\right)^\alpha \sum_{l=0}^j 3^{-l}\omega_l\omega_{j-l}$, where ω_l are the coefficients of the Grünwald–Letnikov formula in (3.14). Using this formula and the asymptotic expansion of the binomial coefficients [36], we have the following more details about the behavior of these coefficients, the asymptotic decay rate $\mu_n = O(n^{-\alpha-1})$ [36] and $\delta_n = O(n^{-\alpha})$.

Lemma 3.10 ([18]). *For $0 < \alpha < 1$, we have*

$$\mu_0 = \left(\frac{3}{2}\right)^\alpha, \ \mu_1 = -\left(\frac{3}{2}\right)^\alpha \frac{4\alpha}{3}, \ \mu_2 = \left(\frac{3}{2}\right)^\alpha \frac{\alpha(8\alpha - 5)}{9},$$

$$\mu_3 = \left(\frac{3}{2}\right)^\alpha \frac{4\alpha(\alpha-1)(7-8\alpha)}{81}; \ \mu_j < 0 \ for \ j \geq 4; \ \sum_{j=0}^\infty \mu_j = 0;$$

$$\mu_n = O(n^{-\alpha-1}) \ \ as \ n \to \infty; \quad \delta_n = O(n^{-\alpha}).$$

3.5.2. Quadratic interpolation approximations

The L1 method can be seen as a linear interpolation formula on each subinterval, and has the accuracy of order $2 - \alpha$ for smooth functions. High order approximations to the Caputo derivative can be constructed by using the multiple nodal interpolations for the integrands. In particular, the quadratic interpolation approximation (QIA) [19,34] gives

$$_0^C D_t^\alpha x(t)|_{t=t_n} = \frac{1}{h^\alpha}\sum_{j=0}^n \mu_{n-j}x_j + O(h^{3-\alpha}) \tag{3.18}$$

for smooth functions. The coefficients $\{\mu_j\}_{j\geq 0}$ were given in [19,34], and have the following properties.

Lemma 3.11 ([34]). *For $n \geq 4$, $0 < \alpha < 1$ and $d_0 = 1/\Gamma(3-\alpha)$, we have*

$$\mu_0 = 2^{1-\alpha}(1+\alpha/2)d_0 > 0, \quad -\frac{4}{3}d_0 < \mu_1 < 0, \quad -\frac{1}{3}d_0 < \mu_2 < \frac{1}{2}d_0,$$

$$\mu_j < 0 \; for \; j \geq 3; \quad \sum_{j=0}^{n} \mu_j = 0; \quad \mu_n = O(n^{-\alpha}) \;\; as \;\; n \to \infty.$$

As we can see from Lemmas 3.10 and 3.11, some weights in the above two methods might be positive, e.g., μ_2, μ_3 in second order F-BDFs, and μ_2 in QIA. This is very different from the previous G–L formula and L1 method, and causes some difficulties for us to derive the energy-like inequality in Lemma 3.2. In [34], a special technique was introduced to transform all the coefficients $\{\mu_j\}_{j\geq 1}$ in QIA to be negative. But the transformation is essentially linear and appears to be difficult to apply to nonlinear systems. However, we are still able to establish the contractivity and dissipativity for these high order schemes by slightly relaxing our previous assumptions, as it is shown in Theorem 3.12.

Theorem 3.12. (i) *Let function f in the F-ODEs (1.1) satisfy the one-sided Lipschitz condition (1.3). Then the second order F-BDFs and QIA are contractive if*

$$h^\alpha \lambda \leq \begin{cases} -2\mu_2 - 2\mu_3, & \text{for second order F-BDFs,} \\ -2\mu_2, & \text{for QIA,} \end{cases} \tag{3.19}$$

and any two different solutions x_n and y_n meet the following contractivity estimate

$$\|x_n - y_n\|^2 \leq \|x_0 - y_0\|^2 \cdot \frac{c_\alpha}{n^\alpha} \;\; as \; n \to \infty. \tag{3.20}$$

(ii) Let function f in (1.1) satisfy the dissipative condition (1.5). Then the second order F-BDFs and QIA are dissipative if

$$h^\alpha b \geq \begin{cases} 2\mu_2 + 2\mu_3, & \text{for second order F-BDFs,} \\ 2\mu_2, & \text{for QIA,} \end{cases} \tag{3.21}$$

i.e., for any initial value x_0 and $\varepsilon > 0$, there is a bounded set $B(0,r)$ and $n_0 \in N^+$ such that $x_n \in B(0,r)$ for all $n \geq n_0$, with $r = \sqrt{c_\alpha a/b} + \varepsilon$. Moreover, if condition (1.5) holds with $a = 0$, the dissipativity is given by $\|x_n\|^2 \leq c_\alpha \|x_0\|^2 n^{-\alpha}$ as $n \to \infty$.

Proof. (i) We prove only the result for the QIA, and the same argument can be used to show the result for the second order F-BDFs. Let $z_n = x_n - y_n$, and take the inner product with $2z_n$ on both sides of the numerical scheme and then apply the one-sided Lipschitz condition to obtain

$$\left\langle \sum_{j=0}^{n} \mu_{n-j} z_j, 2z_n \right\rangle = 2h^\alpha \langle f(x_n) - f(y_n), z_n \rangle \leq 2h^\alpha \lambda \|z_n\|^2. \tag{3.22}$$

Without loss of generality, we assume $n \geq 4$. We know from Lemma 3.11 that only the coefficient μ_2 may be positive. If $\mu_2 \leq 0$, the results follow as in the proof of Theorem 3.4. We now prove for the case that $\mu_2 > 0$. Define the new weights $\{\tilde{\mu}_j\}_{j\geq 0}$: $\tilde{\mu}_0 = \mu_0 + \mu_2$, $\tilde{\mu}_1 = \mu_1$, $\tilde{\mu}_2 = 0$ and $\tilde{\mu}_j = \mu_j$ for $j \geq 3$. Then the inequality (3.22) can be written as

$$\left\langle \sum_{j=0}^{n} \tilde{\mu}_{n-j} z_j, 2z_n \right\rangle + \mu_2 \langle z_{n-2} - z_n, 2z_n \rangle \leq 2h^\alpha \lambda \|z_n\|^2. \tag{3.23}$$

We can now check that $\tilde{\mu}_0 > 0$, $\tilde{\mu}_j \leq 0$ for all $j \geq 1$ and that $\sum_{j=0}^{n} \tilde{\mu}_j \geq 0$ for $n \geq 1$. Now Lemma 3.2 and the Cauchy inequality yields that $\sum_{j=0}^{n} \tilde{\mu}_{n-j}\|z_j\|^2 - 3\mu_2\|z_n\|^2 - \mu_2\|z_{n-2}\|^2 \leq 2h^{\alpha}\lambda\|z_n\|^2$. This inequality is equivalent to

$$\|z_n\|^2 \leq \frac{1}{\tilde{\mu}_0 - 3\mu_2 - 2h^{\alpha}\lambda} \left(\sum_{j=0}^{n-1} |\tilde{\mu}_{n-j}| \, \|z_j\|^2 + \mu_2\|z_{n-2}\|^2 \right). \tag{3.24}$$

Now the assumption $h^{\alpha}\lambda < -2\mu_2$ ensures that

$$\rho_3 = \frac{1}{\tilde{\mu}_0 - 3\mu_2 - 2h^{\alpha}\lambda} \left(\sum_{j=0}^{n-1} |\tilde{\mu}_{n-j}| + \mu_2 \right) = \frac{\mu_0 + 2\mu_2}{\mu_0 - 2\mu_2 - 2h^{\alpha}\lambda} < 1, \text{ for any } n \geq 1. \tag{3.25}$$

Then the estimate (3.20) follows from Lemma 3.3.

(ii) The same as in part (i), we introduce the new weights $\{\tilde{\mu}_j\}_{j \geq 0}$ and can then derive using the dissipative condition,

$$\left\langle \sum_{j=0}^{n} \tilde{\mu}_{n-j}x_j, 2x_n \right\rangle + \mu_2 \langle x_{n-2} - x_n, 2x_n \rangle \leq 2h^{\alpha} \left(a - b\|x_n\|^2 \right). \tag{3.26}$$

By Lemma 3.2 and the Cauchy inequality, we can further deduce

$$\|x_n\|^2 \leq \frac{1}{\tilde{\mu}_0 - 3\mu_2 + 2h^{\alpha}b} \left(2h^{\alpha}a + \sum_{j=0}^{n-1} |\tilde{\mu}_{n-j}| \|x_j\|^2 + \mu_2\|x_{n-2}\|^2 \right). \tag{3.27}$$

Now the assumption $h^{\alpha}b > 2\mu_2$ ensures that

$$\rho_4 = \frac{1}{\tilde{\mu}_0 - 3\mu_2 + 2h^{\alpha}b} \left(\sum_{j=0}^{n-1} |\tilde{\mu}_{n-j}| + \mu_2 \right) = \frac{\mu_0 + 2\mu_2}{\mu_0 - 2\mu_2 + 2h^{\alpha}b} < 1 \text{ for any } n \geq 1. \tag{3.28}$$

Then we can see the desired dissipativity follows from Lemma A.1 or the discrete Paley–Wiener theorem. The dissipativity decay for $a = 0$ can be derived similarly. $\square$

Remark 3.13. The conditions in (3.19) and (3.21) are automatically fulfilled when the weights of the numerical schemes are negative. This is the case with both the G–L formula and L1 method. When the weight coefficients are positive, the constraints in (3.19) and (3.21) are not very restrictive, because the weights μ_2 in QIA or $\mu_2 + \mu_3$ in second order F-BDF are usually small, no more than 0.5 which can be verified by direct calculations. So these conditions are relatively easy to meet. We note that these constraints are only sufficient, and it is unclear if they are also necessary.

Remark 3.14. For many other high order F-BDFs in the literature, such as the convolution quadrature type schemes based on high order BDFs or Runge–Kutta methods [36] and the product integration type schemes based on high order interpolation formulas [5], their weights $\{\mu_j\}_{j=0}^{\infty}$ often satisfy the conservation property $\sum_{j=0}^{\infty} \mu_j = 0$ and $\mu_0 > 0$. If there exist k weights from $\{\mu_j\}_{j \geq 1}$ that are positive, say $\mu_{i_1}, \mu_{i_2}, \ldots, \mu_{i_k}$, we may naturally modify the condition in (3.19) to $h^{\alpha}\lambda \leq -2(\mu_{i_1} + \mu_{i_2} + \ldots + \mu_{i_k})$, then the contractivity of F-BDFs can be derived. The dissipativity can also be obtained in a similar manner. However, we like to point out that it is generally difficult to achieve the optimal convergence order of high order methods for F-ODEs due to the low regularity of the true solutions near the initial time. In order to restore the optimal convergence order, some special correction techniques are usually needed, but mostly only a few steps are required near the initial time; see the correction techniques for fractional BDFs in [26], for L1 methods in [48] and for QIA in [45]. These corrections usually do not affect the stability of numerical solutions and the qualitative behaviour of numerical solutions in a long time, nor do they affect the dissipativity and contractivity that are studied in the current work.

4. Numerical experiments

In this section, several numerical examples are presented to validate our theoretically predicted contractivity and dissipativity of the implicit F-BDFs (3.1), and to reveal the algebraic decay rates of the F-ODEs. We will compare the numerical performance of F-BDFs with the popular predictor-corrector type methods, *i.e.*, fractional Adams-Bashforth-Moulton (F-ABM) method, which was proposed in [14], especially for stiff problems.

4.1. Fractional Lorenz system

Consider the system

$$\begin{cases} {}^C_0 D_t^\alpha x_1(t) = x_3 + (x_2 - c_1)x_1, \\ {}^C_0 D_t^\alpha x_2(t) = 1 - c_2 x_2 - x_1^2, \\ {}^C_0 D_t^\alpha x_3(t) = -x_1 - c_3 x_3, \end{cases} \tag{4.1}$$

where c_1, c_2 and c_3 are positive parameters and $c_2 > 1/2$. This example contains many well-known dynamical systems such as the Lorenz, Chen, Chua systems and the financial system [39]. The classical Lorenz system was proved to be dissipative [23] for $\alpha = 1$. Let $x = (x_1, x_2, x_3)^T$, then we have by simple calculations that

$$\begin{aligned} \langle f(x), x \rangle &= -c_1 x_1^2 - c_2 x_2^2 - c_3 x_3^2 + x_2 \\ &\le \frac{1}{2} - c_1 x_1^2 - \left(c_2 - \frac{1}{2}\right) x_2^2 - c_3 x_3^2 \\ &\le a - b\|x\|^2, \end{aligned} \tag{4.2}$$

with $a = 1/2$, $b = \min\{c_1, c_2 - 1/2, c_3\}$. Thus the system is dissipative, and the set $B(0, \sqrt{a/b} + \varepsilon)$ is absorbing.

Figures 1 and 2 plot the numerical solutions computed by the G–L formula and second F-BDFs respectively with various parameters and fractional order α. They show that the order α heavily affect the shape and size of the absorbing set, but all the computed solutions are kept inside the ball $B(0, \sqrt{a/b})$ when the time t increases, as expected. Comparing Figure 1 with Figure 2, we can see that when b is greater (*i.e.*, the conditions in (3.21) is satisfied), the solution has stronger dissipation characteristics, which shrinks to the absorbing set $B(0, \sqrt{a/b})$ at a faster rate. For the L1 method or QIA, similar numerical results are observed but not provided here.

In [43], the F-ABM method was employed to simulate this system. In order to keep the stability, the step size h is required such that $h < h_0(\alpha)$ for some $h_0(\alpha) > 0$. Moreover, when the order α is small, this limitation usually becomes very demanding and can not be used for long time computation. As a comparison, we list in Table 1 the step size limits that make the F-ABM method to be stable. For $\alpha = 0.1$, the step sizes have to be selected about $h = 1e-13$, and the numerical blowup appears for $h = 2e-13$. But the F-BDFs method is stable uniformly for any $h > 0$ and $\alpha \in (0, 1)$. In fact, we guess that there exists certain equivalence relation between
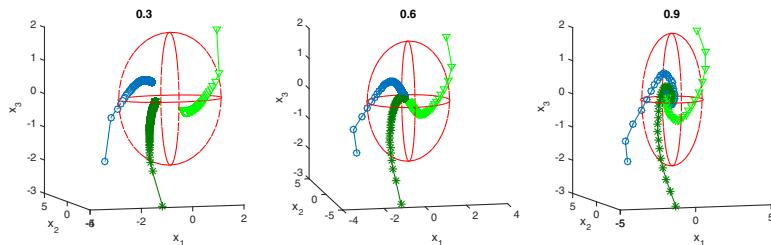
FIGURE 1. Numerical solutions for $\alpha = 0.3, 0.6$ and 0.9 with parameters $c_1 = 1/4, c_2 = 1, c_3 = 1/4$, $a = 1/2, b = 1/4$ and the reference ball $B(0, \sqrt{2})$. Three orbits are computed by G–L method with $h = 0.2$ and $T = 100$ form initial values $(2, 1, 2)^T, (-2, 3, -2)^T$ and $(-1, -4, -3)^T$, respectively.
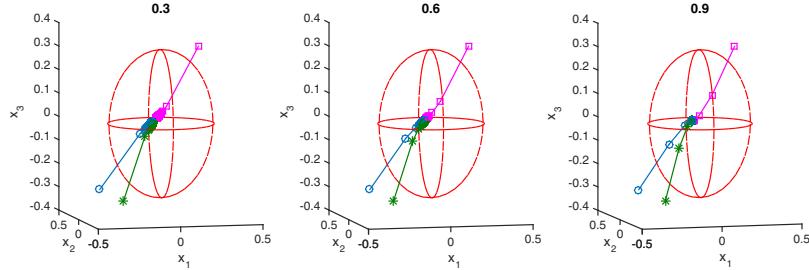
FIGURE 2. Numerical solutions for $\alpha = 0.3, 0.6$ and 0.9 with parameters $c_1 = 5, c_2 = 6, c_3 = 5$, $a = 1/2, b = 5$ and the reference ball $B(0, 1/\sqrt{10})$. Three orbits are computed by second order F-BDFs with $h = 0.4$ and $T = 200$ from the initial values $(0.3, 0.3, 0.3)^T, (-0.3, 0.3, -0.3)^T$ and $(-0.3, -0.3, -0.3)^T$, respectively.

TABLE 1. Numerical performances of the F-ABM for Example 4.1.

	$\alpha = 0.9$	$\alpha = 0.7$	$\alpha = 0.5$	$\alpha = 0.3$	$\alpha = 0.1$
Blowup h	5e-2	2e-2	4e-3	1e-4	2e-13
Stable h	4e-2	1e-2	3e-3	5e-5	1e-13

linear stability and numerical dissipativity for F-ODEs. Hill proved the corresponding equivalence theorem for classical ODEs in [22].

4.2. Fractional sub-diffusion equation

Consider the 2D fractional sub-diffusion equation

$$\begin{cases} {}^C_0D^\alpha_t u(t,x,y) = k\left(u_{xx}(t,x,y) + u_{yy}(t,x,y)\right) + g(t,x,y), \ (x,y) \in \Omega, \\ u(0,x,y) = u_0(x,y), \\ u(t,x,y) = 0, \ (x,y) \in \partial\Omega, \end{cases} \tag{4.3}$$

where $\Omega = [0,1]^2$ and the diffusion coefficient $k > 0$. Applying the standard finite element method with rectangular grids in the spatial direction, we get the F-ODEs

$$ {}^C_0D^\alpha_t U(t) = -kAU(t) + G(t), \tag{4.4}$$

where $U(t), G(t) \in R^{N_x \cdot N_y}$, and N_x, N_y are the numbers of nodes in the x, y-directions respectively. It is well-known that the stiffness matrix A is similar to a symmetric positive matrix, *i.e.*, $D = P^{-1}AP$, where P is an orthogonal matrix. Hence, its eigenvalues are positive and real, *i.e.*, $0 < \lambda_1 \leq \lambda_2 \leq \ldots \leq \lambda_{N_x \cdot N_y}$. Let $F(U) = -kAU(t) + G(t)$. By direct calculations we have

$$\begin{aligned} \langle F(U) - F(V), U - V \rangle &= -k(U-V)^T A(U-V) \\ &= -k(U-V)^T PDP^{-1}(U-V) \\ &\leq \mu\|U-V\|^2, \end{aligned} \tag{4.5}$$

where $\mu = -k\lambda_1 < 0$. Therefore, the F-ODEs (4.4) satisfy the one-sided Lipschitz condition (1.3), and they are contractive. From (1.10), we have the contractivity rate

$$\|U(t) - V(t)\|^2 \leq \|U(0) - V(0)\|^2 \cdot \frac{c_\alpha}{t^\alpha}, \quad c_\alpha > 0. \tag{4.6}$$
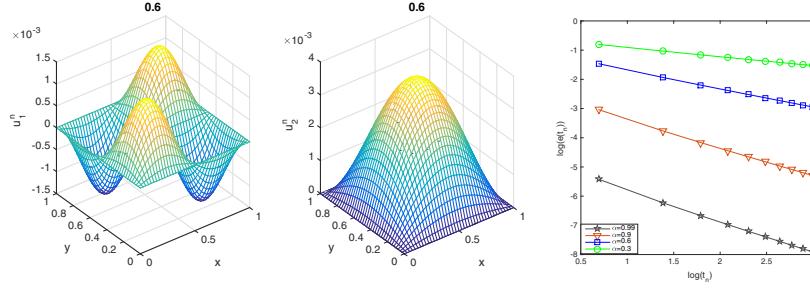
FIGURE 3. Numerical solutions obtained by L1 method at $T = 20$ for $h = 0.2, \alpha = 0.6$ with initial values u_1 and u_2, and the corresponding difference function $e(t)$ on $[0, 100]$ for $h = 0.2$ with $\alpha = 0.3, 0.6, 0.9$ and 0.99.

TABLE 2. The observed index functions p_α by L1 method for Example 4.2 with $h = 0.2$.

t	$\alpha = 0.3$	$\alpha = 0.6$	$\alpha = 0.9$	$\alpha = 0.99$
20	0.3286	0.6771	1.0769	1.4751
40	0.3233	0.6641	1.0461	1.3866
60	0.3209	0.6582	1.0324	1.3481
80	0.3195	0.6546	1.0240	1.3249
100	0.3185	0.6521	1.0182	1.3089

where $U(0), V(0)$ are two given initial values. Since A is symmetric and positive in the semi-discrete system (4.4), it can be diagonalized, so the contractivity rate can be improved to be

$$\|U(t) - V(t)\| \leq \|U(0) - V(0)\| \cdot \frac{c_\alpha}{t^\alpha}, \quad c_\alpha > 0. \tag{4.7}$$

In the numerical simulation, we take the initial values $u_0^1 = \sin(2\pi x)\sin(2\pi y)$, $u_0^2 = 10xy(1 - x)(1 - y)$ and $g(t, x, y) = 0$. Let $e(t) = \|U(t) - V(t)\|$, then the discrete l^2-norm is given by $e(t_n) = \left(\frac{1}{N_x \cdot N_y} \sum_{k=1}^{N_x \cdot N_y} |U_k^n - V_k^n|^2\right)^{\frac{1}{2}}$. Figure 3 reports the numerical solutions and corresponding function $e(t)$ for various fractional order α obtained by L1 method with initial values u_1^0 and u_2^0. It clearly shows that the decay rate of $e(t)$ depends directly on the fractional order parameter α. The greater the order α, the faster the difference function $e(t)$ contracts. But all the contractivity rates remain to be algebraic, rather than the exponential decay rate in the case of integer-order ODEs ($\alpha = 1$).

In order to further analyze the quantitative behavior of the decay rate of $e(t)$, we introduce the index:

$$p_\alpha(t) = \frac{\ln\left(c_\alpha\|U(0) - V(0)\|\right) - \ln\left(\|U(t) - V(t)\|\right)}{\ln(t)}, \quad t > 1 \tag{4.8}$$

from the improved contractivity rate estimation (4.7). Obviously, the index $p_\alpha(t) \to \frac{-\ln(\|U(t) - V(t)\|)}{\ln(t)}$ as $t \to \infty$ and is independent of the initial value $c_\alpha\|U(0) - V(0)\|$. In the numerical simulations, we just take $\|U(1) - V(1)\| = c_\alpha\|U(0) - V(0)\|$.

The observed index p_α for L1 method is presented in Table 2 and for QIA method is given in Table 3. The results show that the contractivity rate is about $\|U(t) - V(t)\| = O(t^{-\alpha})$ as $t \to +\infty$, which is consistent with the continuous estimate in (4.7) and our theoretical prediction for numerical contravtivity rate given in Theorem 3.7.

TABLE 3. The observed index functions p_α by QIA for Example 4.2 with $h = 0.2$.

t	$\alpha = 0.3$	$\alpha = 0.6$	$\alpha = 0.9$	$\alpha = 0.99$
20	0.3451	0.6768	0.8355	1.7972
40	0.3375	0.6639	0.8498	1.6480
60	0.3341	0.6581	0.8555	1.5835
80	0.3320	0.6546	0.8587	1.5449
100	0.3305	0.6521	0.8609	1.5182
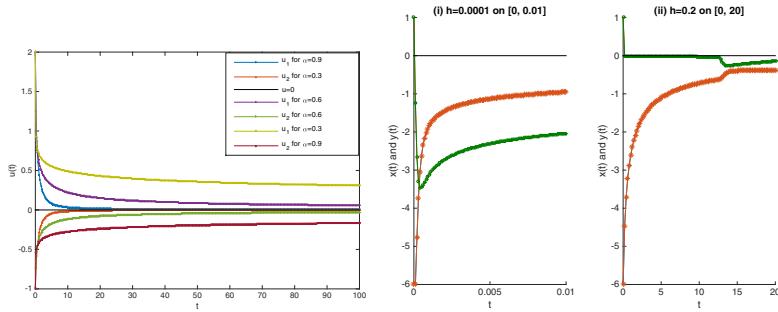
FIGURE 4. Left: numerical solutions of (i) at $T = 100$ obtained by G–L with $h = 0.2$, initial values $u_1 = 2$, $u_2 = -1$ and $\alpha = 0.3, 0.6, 0.9$; Middle: numerical solutions of (ii) at $T = 0.01$ obtained by L1 with $h = 0.0001$ on $[0, 0.01]$ with $\alpha = 0.6$ and initial values $x_0 = -6, y_0 = 1$; Right: numerical solutions of (ii) at $T = 20$ obtained by L1 with $h = 0.2$ on $[0, 20]$ with $\alpha = 0.6$ and initial values $x_0 = -6, y_0 = 1$.

The semi-discrete F-ODEs (4.4) is stiff when t is small, and F-BDFs work well for relatively large step size $h = 0.2$. As a comparison, when we make use of the F-ABM method proposed in [14] for simulations, numerical blowup or oscillation appears even for $h = 1e - 14$ when $\alpha = 0.3$. The serious restrictions on the step sizes, especially when α is small, indicate that the explicit F-ABM method is not suitable for stiff F-ODEs. In fact, the linear stability of fractional predictor-corrector methods was studied deeply in [17], and it was shown that the stability regions of this type of methods are usually relatively small, not suitable for stiff F-ODEs.

4.3. Nonlinear F-ODEs

Consider the nonlinear F-ODEs

$$(i) \begin{cases} {}^{C}_{0}D^\alpha_t x(t) = -x^3 - x, \\ x(0) = x_0. \end{cases} \quad (ii) \begin{cases} {}^{C}_{0}D^\alpha_t x(t) = -10xy^2 - x, \\ {}^{C}_{0}D^\alpha_t y(t) = 10x^2y - y, \end{cases} \tag{4.9}$$

By simple calculations, it is easy to check that scalar F-ODEs in (i) satisfy the one-sided Lipschitz condition with $\lambda = -1$, and also meet the dissipative condition with $a = 0, b = 1$. Hence, it is contractive and dissipative. The F-ODEs in (ii) satisfy the dissipative condition with $a = 0, b = 1$, hence are dissipative.

From Figure 4, we find that the sign of the numerical solution in scalar F-ODEs (i) remains unchanged, as shown in Lemma 3.6. The order α significantly affects the contractivity rate and dissipativity rate, and all the solutions decay to zero at a slow rate and keep a long tail. As in Example 4.2, we can compute the index p_α defined in (4.8) to quantitatively characterize the contractivity rate. Tables 4 and 5 show that the contractivity rate depends directly on the order parameter α and is algebraic, and almost equal to the rate α, which is consistent with the results presented in Theorem 3.7. Note that when $\alpha = 0.3$, the index p_α is slightly smaller

TABLE 4. Observed index function p_α in Example 4.3 (i) computed by G–L with $h = 0.5$ and $T = 5000$.

t	$\alpha = 0.3$	$\alpha = 0.6$	$\alpha = 0.9$	$\alpha = 0.99$
1000	0.2149	0.5682	1.0672	1.4874
2000	0.2200	0.5714	1.0520	1.4739
3000	0.2228	0.5729	1.0441	1.4101
4000	0.2247	0.5739	1.0390	1.3906
5000	0.2262	0.5746	1.0352	1.3755

TABLE 5. Observed p_α in Example 4.3 (i) computed by second order F-BDFs with $h = 0.5$ and $T = 5000$.

t	$\alpha = 0.3$	$\alpha = 0.6$	$\alpha = 0.9$	$\alpha = 0.99$
1000	0.2333	0.6036	1.1183	1.5437
2000	0.2367	0.6035	1.0984	1.4884
3000	0.2387	0.6035	1.0882	1.4601
4000	0.2407	0.6034	1.0817	1.4397
5000	0.2412	0.6034	1.0767	1.4250

TABLE 6. The observed index function q_α in Example 4.3 (ii) computed by L1 with $h = 0.5$ and $T = 5000$.

t	$\alpha = 0.3$	$\alpha = 0.6$	$\alpha = 0.9$	$\alpha = 0.99$
1000	0.2662	0.6038	1.1094	1.5342
2000	0.2678	0.6037	1.1090	1.4830
3000	0.2639	0.6036	1.1080	1.4552
4000	0.2613	0.6035	1.1074	1.4362
5000	0.2596	0.6035	1.1069	1.4246

than expected because it takes a long time to get to the equilibrium. For long time simulations, some fast algorithm for Caputo derivatives, should be very helpful.

From Figure 4, we see that the sign of the numerical solutions in the vector F-ODEs (ii) is no longer unchanged. It also exhibits an initial layer and thus has a stiff feature. We now introduce an index to quantitatively characterize the dissipativtity rate:

$$q_\alpha(t) = \frac{\ln\left(c_\alpha \|u(0)\|\right) - \ln\left(\|u(t)\|\right)}{\ln(t)}, \quad t > 1. \tag{4.10}$$

The index $q_\alpha(t) \to \frac{-\ln(\|u(t)\|)}{\ln(t)}$ as $t \to +\infty$ and is also independent of the initial values $c_\alpha \|u(0)\|$. In the numerical simulations, we just take $\|u(1)\| = c_\alpha \|u(0)\|$. Table 6 shows that the dissipativity rate depends directly on the order α and is algebraic, with the rate nearly equal to α.

5. Concluding remarks

We have presented some sufficient conditions to ensure the numerical contractivity and dissipativity of F-BDFs for nonlinear F-ODEs. F-BDFs, including four popular schemes, are shown to be dissipative and contractive,

and can preserve the exact contractivity and dissipativity rates of the solutions to the continuous equations. To the best of our knowledge, this is the first work on the numerical asymptotic behavior of the solutions to nonlinear F-ODEs. There are still a lot to be done in order to better understand efficient numerical methods for nonlinear F-ODEs without the classical Lipschitz conditions. For instance, stable numerical methods for strongly stiff F-ODEs and their rigorous long-time convergence analysis are very important.

We note that for Riemann–Liouville F-ODEs, the numerical dissipativity and contractivity of the F-BDFs that we have studied can be developed directly. But the decay rate for Riemann–Liouville F-ODEs is slightly changed. For the multi-order fractional systems with $\alpha = (\alpha_1, \alpha_2, \ldots, \alpha_n)^T$, where $\alpha_i \in (0, 1)$ for $i = 1, 2, \ldots, n$, their numerical dissipativity and contractivity of F-BDFs can be established in a similar manner.

APPENDIX A. ASYMPTOTICAL DECAY RATE OF VOLTERRA DIFFERENCE EQUATION

We introduce some related concepts and results in [2]. Let $r > 0$ be finite. A real sequence $\gamma = \{\gamma_n\}_{n \geq 0}$ is in $W(r)$ if $\gamma_n > 0$ and

$$\lim_{n \to \infty} \frac{\gamma_{n-1}}{\gamma_n} = \frac{1}{r}, \ \tilde{\gamma}(r) = \sum_{i=0}^{\infty} \gamma_i r^{-i} < \infty \quad \text{and} \quad \lim_{m \to \infty} \left(\limsup_{n \to \infty} \frac{1}{\gamma_n} \sum_{i=m}^{n-m} \gamma_{n-i} \gamma_i \right) = 0.$$

Note that if $\gamma \in W(r)$ and $r \leq 1$, then $\lim_{n \to \infty} \gamma_n = 0$ as $n \to \infty$. The sequence $\gamma_n = 1/(n+1)^{1+\alpha} \in W(1)$ while $\gamma_n = 1/(n+1)^\alpha$ is not in $W(1)$ for $0 < \alpha < 1$. For a given sequence $\gamma = \{\gamma_n\}_{n \geq 0}$ in $W(r)$ and $x = \{x_n\}_{n \geq 0}$, we define $L_\gamma(x) = \lim_{n \to \infty} \frac{x_n}{\gamma_n}$ if the limit exists. We now recall the main results of [2] in the scalar case.

Lemma A.1 ([2]). *Consider the Volterra difference equation*

$$z_{n+1} = h_n + \sum_{i=0}^{n} H_{n,i} z_i, \quad n \geq 1. \tag{A.1}$$

Assume that

(i) $K := \lim_{m \to \infty} \sup_{m \geq 0} \left(\limsup_{n \to \infty} \sum_{j=0}^{m} |H_{n,n-j}| \right)$ *is finite with $K < 1$;*

(ii) $H_{n,m} \sim H_{\infty,m}$ *and* $h_n \sim h_\infty$ *as* $n \to \infty$ *with* $\sum_{m=0}^{\infty} |H_{\infty,m}| < \infty$;

(iii) $\lim_{m \to \infty} \left(\limsup_{n \to \infty} \sum_{j=m}^{n-m} |H_{n,j}| \right) = 0.$

Then the limit $\lim_{n \to \infty} z_n$ exists and satisfies

$$\lim_{n \to \infty} z_n = (1 - V)^{-1} \left(h_\infty + \sum_{j=0}^{\infty} H_{\infty,j} z_j \right) \quad \text{with} \quad V := \lim_{m \to \infty} \left(\lim_{n \to \infty} \sum_{j=0}^{m} H_{n,n-j} \right). \tag{A.2}$$

Furthermore, when (A.1) is a convolution equation with $H_{n,j} = H_{n-j}^\sharp$ and $\sum_{j=0}^{\infty} |H_j^\sharp| < 1$, it is seen that $K = \sum_{j=0}^{\infty} |H_j^\sharp| < 1$, $V = \sum_{j=0}^{\infty} H_j^\sharp$ and $H_\infty = 0$. Therefore, the limit $\lim_{n \to \infty} z_n$ exists and satisfies

$$\lim_{n \to \infty} z_n = \left(1 - \sum_{j=0}^{\infty} H_j^\sharp \right)^{-1} h_\infty. \tag{A.3}$$

References

[1] A.A. Alikhanov, A priori estimates for solutions of boundary value problems for fractional-order equations. *Differ. Equ.* **46** (2010) 660–666.

[2] J.A.D. Appleby, I. Győri and D.W. Reynolds, On exact convergence rates for solutions of linear systems of Volterra difference equations. *J. Diff. Equa. Appl.* **12** (2006) 1257–1275.

[3] J.C. Butcher, A stability property of implicit Runge–Kutta methods. *BIT Numer. Math.* **15** (1975) 358–361.

[4] J.C. Butcher, Thirty years of G-stability. *BIT Numer. Math.* **46** (2006) 479–489.

[5] J. Cao, C. Li and Y.Q. Chen, High-order approximation to Caputo derivatives and Caputo-type advection-diffusion equations (II). *Fract. Calc. Appl. Anal.* **18** (2015) 735–761.

[6] W. Cao, Z. Zhang and G.E. Karniadakis, Time-splitting schemes for fractional differential equations I: smooth solutions. *SIAM J. Sci. Comput.* **37** (2015) A1752–A1776.

[7] W. Cao, F. Zeng, Z. Zhang and G.E. Karniadakis, Implicit-explicit difference schemes for nonlinear fractional differential equations with nonsmooth solutions. *SIAM J. Sci. Comput.* **38** (2016) A3070–A3093.

[8] J. Čermák, I. Győri and L. Nechvátal, On explicit stability conditions for a linear fractional difference system. *Fract. Calc. Appl. Anal.* **18** (2015) 651–672.

[9] E. Cuesta, Asymptotic behaviour of the solutions of fractional integro-differential equations and some time discretizations. *Discrete Contin. Dyn. Syst.* (2007) 277–285.

[10] E. Cuesta, C. Lubich and C. Palencia, Convolution quadrature time discretization of fractional diffusion-wave equations. *Math. Comput.* **75** (2006) 673–696.

[11] G. Dahlquist, Error analysis for a class of methods for stiff nonlinear initial value problems. In: Vol. 506 of *Numerical Analysis, Lecture Notes in Mathematics*. Springer Berlin Heidelberg (1975) 60–74.

[12] G. Dahlquist, G-stability is equivalent to A-stability. *BIT Numer. Math.* **18** (1978) 384–401.

[13] K. Diethelm and N.J. Ford, Analysis of fractional differential equations. *J. Math. Anal. Appl.* **265** (2002) 229–248.

[14] K. Diethelm, N.J. Ford and A.D. Freed, A predictor–corrector approach for the numerical solution of fractional differential equations. *Nonlinear Dyn.* **29** (2002) 3–22.

[15] P.P.B. Eggermont, Uniform error estimates of Galerkin methods for monotone Abel–Volterra integral equations on the half-line. *Math. Comput.* **53** (1989) 157–189.

[16] L. Galeone and R. Garrappa, On multistep methods for differential equations of fractional order. *Mediterr. J. Math.* **3** (2006) 565–580.

[17] R. Garrappa, On linear stability of predictor-corrector algorithms for fractional differential equations. *Int. J. Comput. Math.* **87** (2010) 2281–2290.

[18] R. Garrappa, Trapezoidal methods for fractional differential equations: theoretical and computational aspects. *Math. Comput. Simul.* **110** (2015) 96–112.

[19] G.H. Gao, Z.Z. Sun and H.W. Zhang, A new fractional numerical differentiation formula to approximate the Caputo fractional derivative and its applications. *J. Comput. Phys.* **259** (2014) 33–50.

[20] E. Hairer and G. Wanner, Solving ordinary differential equations II, 2nd edition. In: Vol. 14 of *Stiff and Differential-Algebraic Equations. Springer Series in Computational Mathematics*. Springer, Berlin (1996).

[21] J.K. Hale, Asymptotic Behavior of Dissipative Systems. American Mathematical Society, New York (2010).

[22] A.T. Hill, Global dissipativity for A-stable methods. *SIAM J. Numer. Anal.* **34** (1997) 119–142.

[23] A.R. Humphries and A.M. Stuart, Runge–Kutta methods for dissipative and gradient dynamical systems. *SIAM J. Numer. Anal.* **31** (1994) 1452–1485.

[24] B. Jin, R. Lazarov and Z. Zhou, An analysis of the L1 scheme for the subdiffusion equation with nonsmooth data. *IMA J. Numer. Anal.* **36** (2016) 197–221.

[25] B. Jin, R. Lazarov, V. Thomée and Z. Zhou, On nonnegativity preservation in finite element methods for subdiffusion equations. *Math. Comput.* **86** (2017) 2239–2260.

[26] B. Jin, B. Li and Z. Zhou, Correction of high-order BDF convolution quadrature for fractional evolution equations. *SIAM J. Sci. Comput.* **39** (2017) A3129–A3152.

[27] B. Jin, B. Li and Z. Zhou, Numerical analysis of nonlinear subdiffusion equations. *SIAM J. Numer. Anal.* **56** (2018) 1–23.

[28] A.A. Kilbas, H.M. Srivastava and J.J. Trujillo, Theory and Applications of Fractional Differential Equations. Elsevier Science Limited, Amsterdam (2006).

[29] N. Kopteva, Error analysis of the L1 method on graded and uniform meshes for a fractional-derivative problem in two and three dimensions. *Math. Comput.* **88** (2019) 2135–2155.

[30] H. Li, J. Cao and C. Li, High-order approximation to Caputo derivatives and Caputo-type advection-diffusion equations (III). *J. Comput. Appl. Math.* **299** (2016) 159–175.

[31] C.P. Li and F.R. Zhang, A survey on the stability of fractional differential equations. *Eur. Phys. J. Spec. Top.* **193** (2011) 27–47.

[32] Y. Li, Y.Q. Chen and I. Podlubny, Mittag–Leffler stability of fractional order nonlinear dynamic systems. *Automatica* **45** (2009) 1965–1969.

[33] Y. Lin and C. Xu, Finite difference/spectral approximations for the time-fractional diffusion equation. *J. Comput. Phys.* **225** (2007) 1533–1552.

[34] C. Lv and C. Xu, Error analysis of a high order method for time-fractional diffusion equations. *SIAM J. Sci. Comput.* **38** (2016) A2699–A2724.

[35] C. Lubich, On the stability of linear multistep methods for Volterra convolution equations. *IMA J. Numer. Anal.* **3** (1983) 439–465.

[36] C. Lubich, Fractional linear multistep methods for Abel–Volterra integral equations of the second kind. *Math. Comput.* **45** (1985) 463–469.

[37] D. Matignon, Stability results for fractional differential equations with applications to control processing. In: Vol. 2 of *Computational Engineering in Systems Applications*. IMACS, IEEE-SMC, Lille, France (1996) 963–968.

[38] O. Nevanlinna, On the numerical solutions of some Volterra equations on infinite intervals. *Math.-Rev. Anal. Numr. Thor. Approx.* **5** (1976) 31–57.

[39] I. Petras, Fractional-order Nonlinear Systems: Modeling, Analysis and Simulation. Higher Education Press, Beijing and Springer-Verlag, Berlin (2011).

[40] I. Podlubny, Fractional Differential Equations. Academic Press, London (1998).

[41] Z. Sun and X. Wu, A fully discrete difference scheme for a diffusion-wave system. *Appl. Numer. Math.* **56** (2006) 193–209.

[42] R. Temam, Infinite dimensional dynamical systems in mechanics and physics. In: Vol. 68 of Applied Mathematical Sciences. Springer-Verlag, Berlin (1998).

[43] D. Wang and A. Xiao, Dissipativity and contractivity for fractional-order systems. *Nonlinear Dyn.* **80** (2015) 287–294.

[44] D. Wang and J. Zou, Dissipativity and contractivity analysis for fractional functional differential equations and their numerical approximations. *SIAM J. Numer. Anal.* **57** (2019) 1445–1470.

[45] Y. Xing and Y. Yan, A higher order numerical method for time fractional partial differential equations with nonsmooth data. *J. Comput. Phys.* **357** (2018) 305–323.

[46] D. Xu, Uniform l^1 behavior for time discretization of a Volterra equation with completely monotonic kernel II: Convergence. *SIAM J. Numer. Anal.* **46** (2008) 231–259.

[47] D. Xu, Decay properties for the numerical solutions of a partial differential equation with memory. *J. Sci. Comput.* **62** (2015) 146–178.

[48] Y. Yan, M. Khan and N.J. Ford, An analysis of the modified L1 scheme for time-fractional partial differential equations with nonsmooth data. *SIAM J. Numer. Anal.* **56** (2018) 210–227.